Gene transfer of two entry inhibitors protects CD4+ T cell from HIV-1 infection in humanized mice

N y Petit, C Baillou, A Burlion, K Dorgham, B Levacher, C Amiel, V Schneider, F M Lemoine, G Gorochov, Gilles Marodon

1 **Gene transfer of two entry inhibitors protects CD4^{+} T cell from HIV-1 infection in**

2 **humanized mice**

3 - Running title: HIV-1 gene therapy in humanized mice

4 Nicolas Y. Petit[1], Claude Baillou[1], Aude Burlion[1], Karim Dorgham[1], Béatrice Levacher[2], Corinne

5 Amiel[1,3], Véronique Schneider[3], François M. Lemoine[1], Guy Gorochov[1,4], Gilles Marodon[1]

6

7 [1] Sorbonne Universités, UPMC Univ PARIS 06, CR7, INSERM U1135, CNRS, Centre

8 d'Immunologie et des Maladies Infectieuses (CIMI), Paris, France

9 [2] Sorbonne Universités, UPMC Univ PARIS 06, CR7, INSERM U959, Paris, France

10 [3] AP-HP, Hôpital Tenon, Service de Virologie, Paris, France

11 [4] AP-HP, Hôpital Pitié-Salpêtrière, Département d'Immunologie, Paris, France

12

13 - The authors declare no conflict of interest.

14 - Corresponding author address: CIMI-PARIS, Bât CERVI, Hôpital Universitaire Pitié-

15 Salpêtrière, 83 Bd de l'Hôpital, 75013 PARIS, FRANCE, tel:+33 14 217 7468 Fax: +33 217

16 7462, email: gilles.marodon@upmc.fr

17

21 **Abstract**

22

23 Targeting viral entry is the most likely gene therapy strategy to succeed in protecting the immune

24 system from pathogenic HIV-1 infection. Here, we evaluated the efficacy of a gene transfer

25 lentiviral vector expressing a combination of viral entry inhibitors, the C46 peptide (an inhibitor

26 of viral fusion) and the P2-CCL5 intrakine (a modulator of CCR5 expression), to prevent CD4$^+$ T

27 cell depletion *in vivo.* For this, we used two different models of HIV-1-infected mice, one in

28 which *ex vivo* genetically-modified human T cells were grafted into immunodeficient

29 NOD.SCID.γc$^{-/-}$ mice before infection and one in which genetically-modified T cells were

30 derived from CD34$^+$ hematopoietic progenitors grafted few days after birth. Expression of the

31 transgenes conferred a major selective advantage to genetically-modified CD4$^+$ T cells, the

32 frequency of which could increase from 10 to 90% in the blood following HIV-1 infection.

33 Moreover, these cells resisted HIV-1-induced depletion, contrary to non-modified cells that were

34 depleted in the same mice. Finally, we report lower normalized viral loads in mice having

35 received genetically-modified progenitors. Altogether, our study documents that targeting viral

36 entry *in vivo* is a promising avenue for the future of HIV-1 gene therapy in humans.

Introduction

Although there is no consensus on a definitive immune correlate of protection, there are multiple convincing examples linking human genetics and susceptibility to HIV-1 infection. The best example of a genetic predisposition protecting from HIV-1 remains the Δ32 mutation that prevents CCR5 expression at the cell surface, and thus completely protects 1% of Europeans from being infected. [1] The so-called 'Berlin patient' was grafted with CCR5-deficient bone marrow to treat his leukemia and was subsequently cured of both diseases. [3] Simultaneously, genetic interventions targeting chemokine receptors using DNA -nucleases gave encouraging results in humanized mice (HuMice) [3–5] but the long term impact of this procedure, as well as the concerns with off-target cleavages, is still unknown. Clinical trials applying this strategy to lymphocytes or stem cells have shown that modified cells possessed a selective advantage compared with non-modified cells, [6] which is one criterion of success for the therapy. Thus, there is a strong rationale to use gene therapy as an adjunct to current and future treatments. [7]

Maraviroc, a CCR5 chemical antagonist, is a powerful medication *in vitro* but resistant variants rapidly emerge in treated patients for complex reasons, such as mutations in the gp120 coding sequence affecting CCR5 docking. [8] Similarly, the fusion inhibitor Enfuvirtide (a gp41 analog), which is delivered in solution to patients, rapidly becomes ineffective because gp41 mutates to escape Enfuvirtide binding. [9] Thus, the therapeutic arsenal targeting viral entry is scarce and poorly efficient. However, strategies based on blocking entry are perhaps the most promising to rapidly restore a pool of functional T cells, the main goal to prevent AIDS. [10] More recently, it was shown that HIV-1 infection needs not to be productive in $CD4^+$ T cells to induce

59 cell death by pyroptosis [11]. This mechanism of HIV-1-induced cell death highlights the interest of

60 strategies aimed at preventing viral entry. We proposed developing a gene transfer vector in

61 which two viral entry inhibitors in combination would have a better efficacy at preventing viral

62 entry. In support of this hypothesis, a synergistic effect of Enfuvirtide was demonstrated in cells

63 with low levels of CCR5 [12]. Importantly, viral variants able to escape gp41 analogs and CCR5

64 inhibitors at the same time have only been described *in vitro* with a drastic cost on viral fitness, [13]

65 illustrating the difficulty for the virus to escape both inhibitors at the same time. Using

66 monocistronic lentiviral vectors, we previously showed a synergistic effect of the P2-CCL5

67 intrakine with the C46 peptide on HIV-1 infection *in vitro* [14]. The P2-CCL5 intrakine, originally

68 described as a high affinity CCL5 (RANTES) variant, [15] was later modified to incorporate an ER

69 retention sequence, sequestering CCR5 away from the cell surface [16]. The C46 peptide is the

70 optimized membrane-bound form of Enfuvirtide and has been used in several gene therapy

71 studies since it is effective on both CCR5- or CXCR4-tropic HIV-1, and can be accommodated in

72 several gene transfer vectors, including lentiviral vectors [17–20]. Here, we aimed to evaluate the *in*

73 *vivo* efficacy of an optimized lentiviral vector co-expressing those two entry inhibitors. We used

74 two pre-clinical models of HIV-1 gene therapy, either infusing genetically-modified T cells in

75 adult immunocompromised NOD.SCID.gc$^{-/-}$ (NSG/PBL) mice or grafting genetically-modified

76 hematopoietic progenitors in NSG neonates (NSG/CD34).

Results

A lentiviral vector expressing two inhibitors of HIV-1 entry

With the general aim to validate the combination of the C46 peptide and the P2-CCL5 intrakine for HIV-1 gene therapy *in vivo*, we used an optimized version of our previously described lentiviral vector, which efficiently inhibited HIV-1 infection *in vitro.*[14] To facilitate detection of genetically-modified cells, we added the GFP reporter gene after the therapeutic cassette to generate the LvGFP-C46-P2 vector (Fig. 1a). A vector using the same strong promoter EF1α but in which the therapeutic cassette was omitted was used as a control (Fig. 1a). We transduced anti-CD3/CD28 activated PBMCs to monitor transgene expression and function *in vitro* and *in vivo*. Expression of the GFP reporter molecule was well correlated with the expression of the C46 peptide (detected with the 2F5 monoclonal antibody) (Fig. 1b) and was also associated with a lower median fluorescence intensity (MFI) of CCR5 *in vitro* (Fig. 1c). Passive diffusion of the intrakine was ruled out by the observation that GFP⁻ cells exhibited similar CCR5 MFI than non-transduced cells (Fig. 1c), suggesting that this reduction was due to ER retention of CCR5 through interaction with the P2-CCL5 intrakine.. The MFI of CCR5 was also reduced two-fold in genetically-modified PBMCs injected *in vivo* in NSG mice (Fig. 1d), reflecting the expected down-modulation of CCR5 surface expression. Thus, GFP expression was a faithful reporter of transgenes expression and function, and was thus used to follow genetically-modified cells *in vivo*.

5

99   *Protection of genetically-modified human CD4$^+$ T cells from HIV-1 infection in NSG/PBL*

100   *mice*

101

102   As a model for HIV-1 infection of human CD4$^+$ T cells *in vivo*, we first used adoptive cell

103   transfer (ACT) in immunocompromised NSG mice (NSG/PBL). A major problem with ACT of

104   human T cells in NSG mice is the xenogeneic graft-versus-host disease (GVHD) that develops

105   thereafter and that invariably leads to death.[21] We tested various ACT protocols in NSG mice and

106   found that injection of 6.10^6 activated T cells in 1 Gy-irradiated mice represented an optimal

107   trade-off between survival and engraftment efficiency (protocol P3 in Figure S1). To normalize

108   the number of genetically-modified cells across experiments and vectors, we diluted transduced

109   cells into non-transduced cells *ex vivo* prior ACT, establishing a number of GFP$^+$ cells at 10% of

110   the injected cells. Mice were infected i.v with a CCR5-tropic HIV-1 strain 12 days after ACT.

111   The frequencies of CD4$^+$GFP$^+$ cells steadily increased in the blood of LvGFP-C46-P2-treated

112   animals during the course of the infection to reach a plateau where up to 95% of all CD4$^+$ T cells

113   expressed the transgene (Fig. 2a). In contrast, the frequencies of GFP$^+$ cells in control HIV-1-

114   infected LvGFP-treated mice remained close to the 10% input throughout the experiment (Fig.

115   2a). The increase in GFP$^+$ cells with the LvGFP-C46-P2 vector was dependent on HIV-1

116   infection because it was not observed in non-infected NSG/PBL mice (Fig. S2), showing that the

117   therapeutic vector did not increase the proliferation of modified cells *per se*. The frequencies of

118   GFP$^+$ cells were also superior in the spleen and in the bone marrow of LvGFP-C46-P2-treated

119   mice compared with LvGFP-treated control mice (Fig. 2b). These increased frequencies

120   translated into increased numbers of CD4$^+$GFP$^+$ cell in the spleen and the bone marrow of

121 LvGFP-C46-P2-treated mice compared with LvGFP mice (Fig. S3). Altogether, the results

122 demonstrate that LvGFP-C46-P2-transduced CD4^{+} T cells possess a selective advantage relative

123 to LvGFP-modified T cells.

124   To test the hypothesis that genetically-modified cells resisted HIV-1-induced depletion,

125 we analyzed longitudinally the frequencies of CD4^{+} cells in CD3^{+}GFP^{+} and CD3^{+}GFP^{-} T cells in

126 the blood of LvGFP-C46-P2- and LvGFP-treated mice (Fig. 2c). The frequencies of CD4^{+} T cells

127 in the GFP^{-} subset rapidly dropped after HIV-1 infection, showing that non-protected CD4^{+} T

128 cells underwent HIV-1-induced depletion as expected (Fig. 2d). In striking contrast, the

129 frequency of CD4^{+} T cells in the GFP^{+} fraction remained constant throughout the experiment,

130 showing that these cells were protected from HIV-1-induced depletion. Resistance to depletion

131 was also observed in the spleen and in the bone marrow of LvGFP-C46-P2-treated animals, with

132 statistically significant differences in the frequencies of CD4^{+} T cells in GFP^{+} vs GFP^{-} T cells

133 (Fig. 2e). In contrast, the frequencies of GFP^{+} cells, like the GFP^{-} subset, steadily decreased in

134 the blood of control LvGFP-treated mice (Fig. S4a), showing that GFP expression *per se* did not

135 protect from HIV-1-induced deletion. A similar depletion of GFP^{+} cells were found in the spleen

136 and in the bone marrow of control LvGFP-treated mice (Fig. S4b). Thus, CD4^{+} T cells expressing

137 the combination of viral entry inhibitors were protected from HIV-1-induced depletion in

138 NSG/PBL mice in the blood and in lymphoid tissues.

139

140 *Resistance of genetically-modified human CD4^{+} T cells to HIV-1-induced depletion in*

141 *NSG/CD34 HuMice*

142

143   We next wanted to confirm the potency of the vector to prevent HIV-1-induced CD4$^+$ T

144   cell depletion in a more physiological setting. For this, we grafted LvGFP-C46-P2-transduced

145   CD34-purified cells from cord blood into neonatal NSG mice and monitored human cell

146   reconstitution and transgene expression overtime. At 17 weeks post-injection, 11.9 ± 11.0 % of

147   total cells from the blood (excluding erythrocytes) were human CD45$^+$CD3$^+$ T cells in the

148   animals used for the experiment. The frequencies of CD4$^+$ and CD8$^+$ T cells among CD3$^+$ cells

149   were less variable representing 40.0 ± 5.8 % and 47.0 ± 5.3 % , respectively (Fig. S5). Among 14

150   NSG/CD34 HuMice generated with LvGFP-C46-P2-modified CD34$^+$ cells, only 8 had detectable

151   GFP$^+$ cells in CD4$^+$ T cells 17 weeks after. Four of those mice were infected with a CCR5-tropic

152   HIV-1 strain, whereas 4 were left uninfected. Because the frequency of GFP$^+$ cells was highly

153   variable among NSG/CD34 HuMice, it was not possible to reliably measure a selective

154   advantage in that setting. To directly assess resistance of genetically-modified CD4$^+$ T cells to

155   HIV-1-induced depletion, frequencies of CD4$^+$ T cells were measured in GFP$^+$ and GFP$^-$ cells

156   (Fig. 3). In non-infected mice, the frequencies of CD4$^+$ T cells in the blood remained similar in

157   GFP$^+$ vs GFP$^-$ T cells throughout the course of the experiment (Fig. 3a). As expected, frequencies

158   of GFP$^-$ cells steadily decreased in HIV-1-infected animals whereas frequencies of GFP$^+$

159   remained stable, showing that CD4$^+$GFP$^+$ T cells resisted HIV-1-induced depletion in the blood

160   of NSG/CD34 HuMice (Fig. 3b). As expected in non-infected mice, the frequencies of CD4$^+$ T

161   cells in lymphoid organs were similar in GFP$^+$ or GFP$^-$ subsets (Fig. 3c). In contrast, frequencies

162   of CD4$^+$ T cells among GFP$^+$ and GFP$^-$ cells significantly differed in the LN, spleen and bone

163   marrow (Fig. 3d). Of note is the one mouse in which resistance to deletion was not evident in the

164   blood did not show any sign of resistance in the lymphoid organs. Thus, gene transfer of two

165   entry inhibitors in CD34$^+$ cells conferred resistance to CD4$^+$ T cells in 3 mice out of 4 analyzed.

166

167

168   *Gene transfer of entry inhibitors impact viral replication in NSG/CD34 HuMice.*

169

170   To assess the impact that the therapy might have on viral loads, we measured viremia in

171   LvGFP-C46-P2-treated mice in which GFP$^+$ cells were observed (n=4) or not (n=6) prior HIV-1

172   infection. To accommodate the various levels of human cells engrafment among the different

173   mice (Fig. S5), viremia was corrected by the frequency of CD45$^+$CD3$^+$CD4$^+$ T cells among total

174   cells of the blood at the time of the analysis. Initially, normalized viremia was similar in both

175   groups, showing that the therapy was not associated with an immediate effect on viral replication.

176   However, we observed a tendency for lower normalized viral loads in mice bearing GFP$^+$ cells

177   compared to mice in which no GFP$^+$ cells could be detected (Fig. 4a). To confirm that animals

178   with GFP$^+$ cells carried less virus, we analyzed p24 expression in CD4$^+$ T cells at the end of the

179   experiment. We found that the frequencies of CD4$^+$ cells expressing p24 in mice with GFP$^+$ cells

180   were lower than in mice without GFP$^+$ cells and close to background staining obtained in non-

181   infected HuMice (Fig. 4b). Altogether, we conclude that NSG/CD34 HuMice reconstituted with

182   gene-modified CD34$^+$ progenitors were protected from HIV-1-induced CD4$^+$ T cell deletion and

183   had a lower number of infected cells, corroborating with lower viral loads.

184   **Discussion**

185

186   Here, we show that a lentiviral vector encoding two viral entry inhibitors confers a

187   selective advantage to genetically-modified cells *in vivo*, due to their resistance to HIV-1-

188   mediated depletion. We observed a strong and long-lasting selective advantage in the NSG/PBL

189   model. A lower selective advantage was reported in a very similar model of NSG/PBL HuMice

190   using a vector expressing only the C46 peptide. [18] This observation suggest that two entry

191   inhibitors might be better than one at protecting cells from HIV-1. However, a pre-clinical study

192   in macaques reconstituted with progenitors expressing the C46 peptide alone showed lower viral

193   loads correlated to a clear selective advantage [22]. Moreover, recent studies showed that inhibition

194   of CCR5 expression by shRNA was sufficient to protect CD4^{+} T cells from infection and to

195   confer a selective advantage in chimeric Bone marrow-Liver-Thymus (BLT) HuMice [23,24]. Thus,

196   targeting gp41 and CCR5 have independently the potential to curb HIV-1 infection, highlighting

197   the interest of using two inhibitors of this crucial step of HIV-1 infection in the same vector.

198   A strong selective advantage is not always associated with lower viral loads. In CD34-

199   reconstituted HuMice, Walker et al. reported that expression of a triple combination of anti-HIV-

200   1 genes did not impact viral replication, although a significant selective advantage was observed.

201   [25] A modest but significant effect on viral loads was reported following CCR5-specific ZFN-

202   mediated modification in NSG/PBL HuMice. [5] However, only one time point was analyzed in

203   that study. A kinetics study showed that the reduction in viral loads using the same technology

204   was much more discrete in NSG/CD34 HuMice despite a considerable selective advantage. [3] Our

205   PCR and p24 data concur to the hypothesis that selective advantage conferred by our vector had

206   an impact on viral replication. Recently, a complete protection from HIV-1 was observed in BLT

207   mice reconstituted with human cells modified with a vector very similar to our, encoding the C46

208   peptide and a shRNA targeting CCR5 [19]. This is the first report showing that viral replication can

209   be totally controlled in humanized mice by gene therapy without prior sorting of genetically-

210   modified cells, as recently shown for a CCR5 shRNA [26]. This surprising and unique result

211   suggest that maximal efficacy of HIV-1 gene therapy might necessitate a functional immune

212   response, that is present in monkeys and BLT HuMice but lacking or severely hampered in other

213   HuMice models. One must keep in mind though that some HIV-1-specific PCR might amplify

214   the vector as well [27]. The use of HIV-1-specific PCR discriminating HIV-1 from the vector such

215   as the one employed in our study should become the gold standard.

216   Considering the recent developments of nucleases that target CCR5 in CD34$^+$ progenitor

217   cells , we believe that residual expression of the molecule such as the one observed with our

218   intrakine, might allow for normal hematopoeisis and circulation of modified-cells while total

219   ablation by genetic means may impact on these processes. Recent advances in lentiviral delivery

220   of ZN finger nucleases might improve specific targeting of the nuclease to mature CD4$^+$ T cells, a

221   protocol that would limit bystander effects [28].

222   The selective advantage of genetically-modified cells would only be obtained in the

223   context of high levels of viral replication. Although ART interruptions have been performed in

224   the past to provoke selective growth of modified cells in small-scale clinical trials for gene

225   therapy, [29,30] an interruption in therapy is not foreseeable in patients in the long term. Gene

226   therapy might thus be particularly suitable for patients experimenting treatment failure with high

227   viral loads.

Materials and Methods

228   **Materials and Methods**

229

230   *Lentiviral vector design and production*

231   Second-generation self-inactivating (SIN) lentiviral vectors were used in this study. [31]

232   The LvGFP-C46-P2 vector was constructed by adding an eGFP gene and 2A sequence upstream

233   of the therapeutic cassette (construction encoding the C46 peptide and P2-CCL5 analog

234   described in Petit et al., 2014) [14] in the backbone of a lentiviral vector carrying the EF1a

235   promoter. As a control, the LvGFP vector expressing GFP only was used. Details on the cloning

236   procedures are available on request. Lentiviral vectors were produced in mycoplasma-free HEK-

237   293T cells, as described previously. [32] Briefly, 23.3 µg of the Δ8.9 packaging plasmid, 30 µg of

238   the vector plasmid, and 10 µg of the vesicular stomatitis virus (VSV)-G envelope were

239   transfected into 15.10^6 cells in T-175 flasks by calcium phosphate precipitation. Vector

240   supernatants were collected 48 hours post-transfection and concentrated by ultrafiltration

241   (Centricon Plus-70; Millipore, Molsheim, France) at 3500 g at 4°C. Viral stocks were kept frozen

242   at -80° C. Viral titers were determined on HEK-293T cells with various concentrations of vector

243   supernatants in the presence of Polybrene (8 µg/mL; Sigma-Aldrich, Saint-Quentin-Fallavier,

244   France). Seventy-two hours after transduction, the percentage of cells expressing the transgenes

245   was determined by flow cytometry and used to calculate a viral titer as the number of infectious

246   particles per milliliter.

247

248   *Mice and humanization*

249 NOD Prkdc^{scid} Il2rg^{tm1Wjl} (NSG) mice (strain ≠05557; Jackson Laboratory, USA) were

250 bred in animal facilities of Centre d'Expérimentation Fonctionnelle (CEF) according to the

251 Jackson Laboratory handling practice specific to that strain. The regional ethical committee on

252 animal experimentation Darwin approved all mouse protocols. Primary human cells were

253 obtained from leukapheresis samples collected from healthy donors at the Etablissement Francais

254 du Sang after informed consent. Cells were grown at a concentration of 1.10^6 cells/mL and

255 activated in RPMI, 10% FCS, penicillin/streptomycin, interleukin-2 (Proleukin, 600 IU/mL;

256 Novartis, Basel, Switzerland), and CD3/CD28 beads (Invitrogen, Carlsbad, CA) at 3 beads per

257 cell. Two days after activation, cells were transduced by spinoculation for 2 hrs at 1000 g at

258 30°C, with the indicated lentiviral vectors at a multiplicity of infection (MOI) of 6 to 8 in the

259 presence of protamine sulfate (2 µg/mL, Sigma). Three days after transduction, 1 Gy-irradiated

260 female 8 to 12-weeks old NSG mice were injected with 6.10^6 cells. Twelve days post-adoptive

261 cell transfer (ACT), mice were infected with 25 ng of p24 of NLAD8 HIV-1 strain in a final

262 volume of 100 µL of 1X PBS. All mice used in this study were randomly assigned to

263 experimental group and cages. Investigator was not blinded to the group allocation during the

264 experiments.

265 Human hematopoietic progenitor cells were obtained from cord blood samples collected

266 from healthy donors after informed consent. Mononuclear cells from human cord blood were

267 isolated by Ficoll density gradient and centrifuged at 200 g during 13 min to remove platelets.

268 Then, CD34$^+$ progenitors were sorted with the human CD34 MicroBeads kit, according to the

269 manufacturer's instructions (Miltenyi). CD34$^+$ cells were incubated at a concentration of 1.10^6

270 cells/mL over night into StemSpan SFEMII medium (StemCell technologies) complemented with

13

271 human recombinant cytokines (IL-6 and TPO at 20 ng/mL; SCF and FLT3-L at 100 ng/mL;

272 Peprotech) and antibiotics. Cells were transduced with the LvGFP-C46-P2 lentiviral vector in

273 StemSpan medium in the presence of cytokines, the proteasome inhibitor MG-132 (1 μM;

274 Sigma), antibiotics and protamine sulfate (8 μg/mL; Sigma). CD34$^+$ cells underwent two rounds

275 of transduction separated by 3 hours incubation at 37°C and 5% CO_2. For each transduction

276 cycle, cells were centrifuged at 1000 g at 30°C for 2 hours with the lentiviral vector at a MOI of

277 15. Twenty-four to 48-hour-old NSG mice were irradiated at 0.9 Gy and grafted with $0.5.10^5$ to

278 $2.5.10^5$ transduced CD34$^+$ cells by the intra-hepatic route. Ten ng of the p24 NL-AD8 HIV-1

279 strain were injected into the retro-orbital sinus of 17 weeks-old mice in a final volume of 100 μL

280 of 1X PBS.

281

282 *HIV-1 production and quantification*

283   HIV-1 molecular clone NL-AD8 was obtained through the AIDS Research and Reference

284 Reagent Program. HIV-1 stocks were prepared with 30 μg of plasmid transfected into 15.10^6

285 mycoplasma-free HEK 293T cells in T-175 flasks by calcium phosphate precipitation. The

286 supernatant was frozen at -80°C and viral titers were quantified by p24 ELISA according to the

287 manufacturer's instructions (Zeptometrix, Buffalo, NY). Mice were bled on ACD (acid-Citrate-

288 Dextrose) anticoagulant and plasma HIV-1 RNA viral loads were measured using the Abbott

289 RealTime HIV-1 RT-PCR assay that do not amplify genomic regions present in lentiviral vectors

290 contrary to the Roche Cobas PCR (our unpublished observations and De Ravin et al [27]). Due to

291 the small volumes of plasma from the mice, a dilution was necessary to reach the volume needed

292 for the assay. Thus, this detection limit varied between 200 and 2000 copies/mL depending on the

293   initial volume of mouse plasma.

294

295   *Flow cytometry*

296   Red blood cells from whole blood were lysed with 4.5 ml of water for 15 s before adding

297   0.5 ml of 10X PBS. Red blood cells from spleen or bone marrow were lysed with ACK buffer

298   (NH_4Cl 0.15 M, KHCO3 10 mM, EDTA 0.1 mM). Cell suspensions were stained with an optimal

299   quantity of antibodies at a concentration of 10^7 cells/mL in a final volume of 100 μL of PBS/FCS

300   3%. Incubation was performed in the dark at 6°C for 20 min. The following anti-human mAbs

301   were used for cell surface staining: CD45 PE-CF594 (clone HI30; catalog number (cat ≠)

302   562279, BD Biosciences) anti-CCR5 Alexa Fluor 647 (HEK/1/85a; cat ≠ 313712, Biolegend),

303   anti-CD4 PerCP (RPA-T4, cat ≠ 300528, Biolegend), anti-CD8 Alexa Fluor 700 (HIT8a, cat ≠

304   300920, Biolegend), CD3 PE-Cy7 (UCHT1, cat≠ 300420, Biolegend). The human IgG1 mAb

305   2F5 specific for a gp41 epitope (cat ≠ AB001, Polymun, Austria) was used to detect the C46

306   peptide. The KC57-RD1 (cat≠ 6604667, Beckman Coulter) antibody was used to detect

307   intracellular p24 after cells were treated with permeabilization buffer (eBioscience, fixation and

308   permeabilization kit). All cell preparations were acquired on an LSRII cytometer (BD) and

309   analyzed with FlowJo software (Tree Star, Portland, OR). The frequencies of positive cells were

310   determined according to the fluorescence minus one (FMO) staining negative control.

311

312   *Statistical analysis*

313   No statistical method was used to assess sample size needed to detect an effect. Except for

314   the NSG/CD34 model, which is a single experiment, all the results shown in this study are

315   compiled from 2 independent experiments. Two-tailed p values indicated on the graphs were

316   calculated with Prism version 6.0 software (GraphPad Software, San Diego, CA), using the

317   unpaired Mann-Whitney test with a confidence interval of 95%. The median value are indicated

318   by horizontal bars on the graphs. Linear and non linear regression analysis were performed using

319   Prism 6.0 to determine whether slopes significantly differed. Plateau with one phase decay

320   association or dissociation equations were used to model the data.

335

336 **Conflict of Interest**

337 The authors declare no conflict of interest

338

339   Supplementary information is available at Gene Therapy's website

340

341   Figure S1. Survival and graft efficiency after ACT of activated and transduced T lymphocytes in

342   NSG/PBL HuMice.

343   Figure S2. Selective advantage for LvGFP-C46-P2-modified CD4$^+$ cells is dependent on HIV-1

344   infection.

345   Figure S3. Resistance to HIV-1-induced deletion in LvGFP-C46-P2-injected NSG/PBL mice.

346   Figure S4. CD4$^+$ T cell deletion in LvGFP-control NSG/PBL mice.

347   Figure S5. Human cell reconstitution in 17 weeks-old in NSG/CD34 humanized mice.

348

349

350

References

1 Martinson JJ, Chapman NH, Rees DC, Liu YT, Clegg JB. Global distribution of the CCR5 gene 32-basepair deletion. *Nat Genet* 1997; **16**: 100–103.

2 Allers K, Hütter G, Hofmann J, Loddenkemper C, Rieger K, Thiel E *et al.* Evidence for the cure of HIV infection by CCR5Δ32/Δ32 stem cell transplantation. *Blood* 2011; **117**: 2791–9.

3 Holt N, Wang J, Kim K, Friedman G, Wang X, Taupin V *et al.* Human hematopoietic stem/progenitor cells modified by zinc-finger nucleases targeted to CCR5 control HIV-1 in vivo. *Nat Biotechnol* 2010; **28**: 839–847.

4 Didigu C a, Wilen CB, Wang J, Duong J, Secreto AJ, Danet-Desnoyers G a *et al.* Simultaneous zinc-finger nuclease editing of the HIV coreceptors ccr5 and cxcr4 protects CD4+ T cells from HIV-1 infection. *Blood* 2014; **123**: 61–9.

5 Perez EE, Wang J, Miller JC, Jouvenot Y, Kim KA, Liu O *et al.* Establishment of HIV-1 resistance in CD4+ T cells by genome editing using zinc-finger nucleases. *Nat Biotechnol* 2008; **26**: 808–816.

6 Tebas P, Stein D, Tang WW, Frank I, Wang SQ, Lee G *et al.* Gene Editing of CCR5 in Autologous CD4 T Cells of Persons Infected with HIV. *N Engl J Med* 2014; **370**: 901–910.

7 Peterson CW, Younan P, Jerome KR, Kiem H-P. Combinatorial anti-HIV gene therapy: using a multipronged approach to reach beyond HAART. *Gene Ther* 2013; **20**: 695–702.

8 Colin P, Bénureau Y, Staropoli I, Wang Y, Gonzalez N, Alcami J *et al.* HIV-1 exploits CCR5 conformational heterogeneity to escape inhibition by chemokines. *Proc Natl Acad Sci U S A* 2013; **110**: 9475–80.

9 Greenberg ML, Cammack N. Resistance to enfuvirtide, the first HIV fusion inhibitor. *J Antimicrob Chemother* 2004; **54**: 333–340.

10 Von Laer D, Hasselmann S, Hasselmann K. Gene therapy for HIV infection: what does it need to make it work? *J Gene Med* 2006; **8**: 658–667.

11 Doitsh G, Galloway NLK, Geng X, Yang Z, Monroe KM, Zepeda O *et al.* Cell death by pyroptosis drives CD4 T-cell depletion in HIV-1 infection. *Nature* 2014; **505**: 509–14.

12 Heredia A, Gilliam B, DeVico A, Le N, Bamba D, Flinko R *et al.* CCR5 density levels on primary CD4 T cells impact the replication and Enfuvirtide susceptibility of R5 HIV-1. *Aids* 2007; **21**: 1317–1322.

13 Anastassopoulou CG, Ketas TJ, Sanders RW, Klasse PJ, Moore JP. Effects of sequence changes in the HIV-1 gp41 fusion peptide on CCR5 inhibitor resistance. *Virology* 2012; **428**: 86–97.

14 Petit N, Dorgham K, Levacher B, Burlion A, Gorochov G, Marodon G. Targeting Both Viral and Host Determinants of Human Immunodeficiency Virus Entry, Using a New Lentiviral

Vector Coexpressing the T20 Fusion Inhibitor and a Selective CCL5 Intrakine. *Hum Gene Ther Methods* 2014; **25**: 232–40.

15 Hartley O, Dorgham K, Perez-Bercoff D, Cerini F, Heimann A, Gaertner H *et al.* Human immunodeficiency virus type 1 entry inhibitors selected on living cells from a library of phage chemokines. *J Virol* 2003; **77**: 6637–6644.

16 Schroers R, Davis CM, Wagner HJ, Chen SY. Lentiviral transduction of human T-lymphocytes with a RANTES intrakine inhibits human immunodeficiency virus type 1 infection. *Gene Ther* 2002; **9**: 889–897.

17 Egelhofer M, Brandenburg G, Martinius H, Schult-Dietrich P, Melikyan G, Kunert R *et al.* Inhibition of Human Immunodeficiency Virus Type 1 Entry in Cells Expressing gp41-Derived Peptides. *J Virol* 2004; **78**: 568–575.

18 Kimpel J, Braun SE, Qiu G, Wong FE, Conolle M, Schmitz JE *et al.* Survival of the Fittest: Positive Selection of CD4+ T Cells Expressing a Membrane-Bound Fusion Inhibitor Following HIV-1 Infection. *PLoS One* 2010; **5**: e12357.

19 Burke BP, Levin BR, Zhang J, Sahakyan A, Boyer J, Carroll M V *et al.* Engineering Cellular Resistance to HIV-1 Infection In Vivo Using a Dual Therapeutic Lentiviral Vector. *Mol Ther Acids* 2015; **4**: e236.

20 Trobridge GD, Wu RA, Beard BC, Chiu SY, Muñoz NM, von Laer D *et al.* Protection of stem cell-derived lymphocytes in a primate AIDS gene therapy model after in vivo selection. *PLoS One* 2009; **4**. doi:10.1371/journal.pone.0007693.

21 King MA, Covassin L, Brehm MA, Racki W, Pearson T, Leif J *et al.* Human peripheral blood leucocyte non-obese diabetic-severe combined immunodeficiency interleukin-2 receptor gamma chain gene mouse model of xenogeneic graft-versus-host-like disease and the role of host major histocompatibility complex. *Clin Exp Immunol* 2009; **157**: 104–118.

22 Younan PM, Polacino P, Kowalski JP, Peterson CW, Maurice NJ, Williams NP *et al.* Positive selection of mC46-expressing CD4+ T cells and maintenance of virus specific immunity in a primate AIDS model. *Blood* 2013; **122**: 179–187.

23 Shimizu S, Ringpis G-E, Marsden MD, Cortado R V, Wilhalme HM, Elashoff D *et al.* RNAi-Mediated CCR5 Knockdown Provides HIV-1 Resistance to Memory T Cells in Humanized BLT Mice. *Mol Ther Nucleic Acids* 2015; **4**: e227.

24 Myburgh R, Ivic S, Pepper MS, Gers-Huber G, Li D, Audigé A *et al.* Lentivector knock-down of CCR5 in hematopoietic stem cells confers functional and persistent HIV-1 resistance in humanized mice. *J Virol* 2015; **89**: 6761–6772.

25 Walker JE, Chen RX, McGee J, Nacey C, Pollard RB, Abedi M *et al.* Generation of an HIV-1-Resistant Immune System with CD34+ Hematopoietic Stem Cells Transduced with a Triple-Combination Anti-HIV Lentiviral Vector. J. Virol. 2012; **86**: 5719–5729.

26 Myburgh R, Ivic S, Pepper MS, Gers-Huber G, Li D, Audigé A *et al.* Lentivector knock-down of CCR5 in hematopoietic stem cells confers functional and persistent HIV-1 resistance in humanized mice. *J Virol* 2015; **89**: 6761–6772.

426 27 De Ravin SS, Gray JT, Throm RE, Spindler J, Kearney M, Wu X *et al.* False-Positive HIV
427   PCR Test Following Ex Vivo Lentiviral Gene Transfer Treatment of X-linked Severe
428   Combined Immunodeficiency Vector. *Mol Ther* 2014; **22**: 244–245.

429 28 Abarrategui-Pontes C, Créneguy A, Thinard R, Fine EJ, Thepenier V, Fournier LRL *et al.*
430   Codon swapping of zinc finger nucleases confers expression in primary cells and in vivo
431   from a single lentiviral vector. *Curr Gene Ther* 2014; **14**: 365–76.

432 29 DiGiusto DL, Krishnan A, Li L, Li H, Li S, Rao A *et al.* RNA-based gene therapy for HIV
433   with lentiviral vector-modified CD34(+) cells in patients undergoing transplantation for
434   AIDS-related lymphoma. *Sci Transl Med* 2010; **2**: 36ra43.

435 30 Podsakoff GM, Engel BC, Carbonaro DA, Choi C, Smogorzewska EM, Bauer G *et al.*
436   Selective survival of peripheral blood lymphocytes in children with HIV-1 following
437   delivery of an anti-HIV gene to bone marrow CD34+ cells. *Mol Ther* 2005; **12**: 77–86.

438 31 Zufferey R, Dull T, Mandel RJ, Bukovsky A, Quiroz D, Naldini L *et al.* Self-inactivating
439   lentivirus vector for safe and efficient in vivo gene delivery. *J Virol* 1998; **98**: 9873–9880.

440 32 Marodon G, Mouly E, Blair EJ, Frisen C, Lemoine FM, Klatzmann D. Specific transgene
441   expression in human and mouse CD4+ cells using lentiviral vectors with regulatory
442   sequences from the CD4 gene. *Blood* 2003; **101**: 3416–3423.

443

Figure Legends

Figure 1. Lentiviral vector design and co-expression of anti-HIV-1 genes and eGFP into a
lentiviral vector. (a) A schematic representation of the structure of the lentiviral vectors used in
the present study is shown. (LTR: long terminal repeat; cppT: central polypurine tract of HIV-1;
EF1α: Elongation factor 1 promoter; C46: membrane-bound form of T20 (C46 peptide); 2A: 2A
sequence of the foot-and-mouth disease virus; P2i: P2-CCL5 intrakine; WPRE: Woodchuck
Hepatitis virus regulatory element; ΔLTR: U3 deleted LTR). Indicated is the reference of the
vector used throughout the study. Not to scale. **(b)** Co-expression of the C46 peptide (detected
with the 2F5 mAb) and of eGFP and **(c)** co-expression of CCR5 and eGFP in human CD4$^+$
PBMC activated by CD3/CD28 beads and IL-2 21 to 29 days post transduction with the LvGFP-
C46-P2 vector (NT: Non-transduced; FMO: fluorescence minus one; MFI: median fluorescence
intensity) **(d)** *In vivo* CCR5 expression on CD45$^+$CD3$^+$CD4$^+$ T cells in GFP$^+$ and GFP$^-$ cells from
non-irradiated NSG mice grafted with 2.10^6 LvGFP-C46-P2 transduced T lymphocytes and
analyzed in the blood and the spleen 34 to 53 days post-graft.

Figure 2. Protection of genetically-modified human CD4$^+$ T cells from HIV-1 infection in
NSG/PBL mice. (a-b) Frequencies of GFP$^+$ cells in human CD45$^+$CD3$^+$CD4$^+$ T cells in the
blood at various days after HIV-1 infection **(a)** and in the spleen or bone marrow (BM) **(b)** 35 to
45 days after injection of LvGFP- or LvGFP-C46-P2-modified T cells in NSG mice. **(c)**
Representative histograms and dot plots showing the gating strategy to determine the frequencies
of CD4$^+$ T cells in GFP$^+$ and GFP$^-$ human CD3$^+$ T cells. **(d-e)** Frequencies of CD4$^+$ cells in the
CD3$^+$GFP$^+$ and CD3$^+$GFP$^-$ populations were determined in LvGFP-C46-P2-injected mice in the
blood at various days after infection **(d)** and in the spleen or bone marrow (BM) **(e)** at the end of
the experiment. The results are compiled from 2 independent experiments using the P3 ACT
protocol (Fig. S1). Non linear regression analysis curve fit are shown. The p value indicate the
significant difference between the two slopes.

Figure 3. Resistance of genetically-modified CD4$^+$ T cells to HIV-1-induced depletion *in vivo*
in NSG/CD34 HuMice. (a) Blood frequencies of CD4$^+$ cells in CD3$^+$GFP$^+$ or CD3$^+$GFP$^-$

473   populations were determined in non-infected (HIV⁻) or **(b)** infected **(HIV⁺)** NSG HuMice at

474   various time points after infection. Linear regression curve fit and p values are depicted on the

475   graphs. n.s = not significant (p>0.05) **(c)** Frequencies of CD4$^+$ cells into CD3$^+$GFP$^+$ or

476   CD3$^+$GFP$^-$ populations in HIV⁻ or **(d)** HIV$^+$ mice in the spleen, the lymph nodes (LN) and the

477   bone marrow (BM) 11 weeks post-infection.

478

479   **Figure 4. Gene transfer of entry inhibitors impacts viral replication in NSG/CD34 HuMice**

480   **(a)** Viral load was measured by qPCR after HIV-1 infection in LvGFP-C46-P2-treated mice with

481   undetectable (-GFP) or detectable GFP$^+$ cells (+GFP) in CD4$^+$ T cells prior to infection. Shown is

482   the viral load value normalized by the frequency of human CD45$^+$CD3$^+$CD4$^+$ T cells present in

483   total cells of the blood sample for each time point. **(b)** Frequencies of p24$^+$ cells in CD4$^+$ T cells

484   from the lymph node of NSG HuMice with (+GFP) or without GFP$^+$ cells (-GFP) 77 days after

485   infection with NL-AD8 HIV-1 (HIV+) or non infected (HIV-). A representative CD4 vs p24

486   staining is shown above each group. One mouse from the (+GFP) group was excluded from the

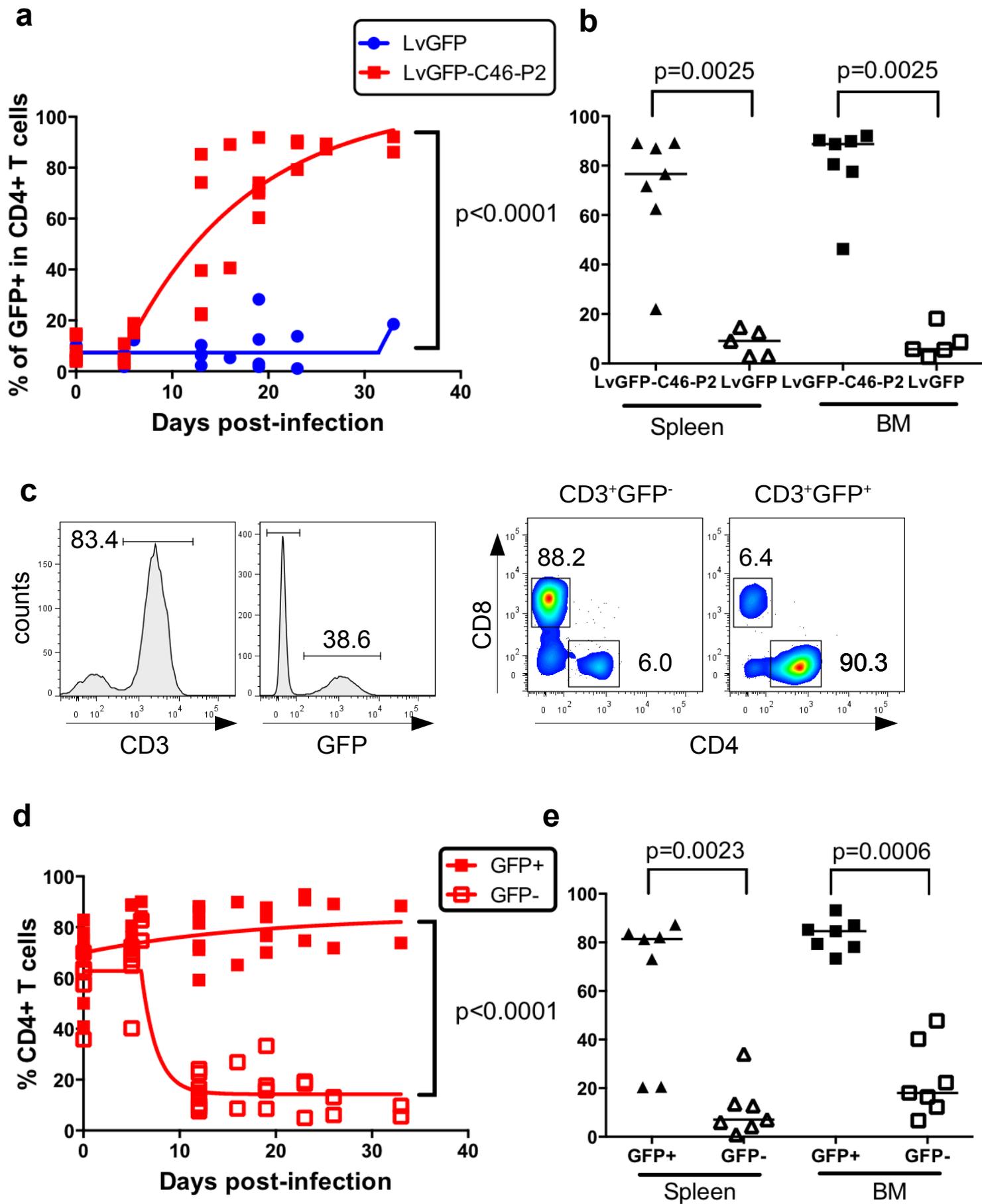487   graph since it did not show any protection against HIV-1-induced depletion in the periphery.
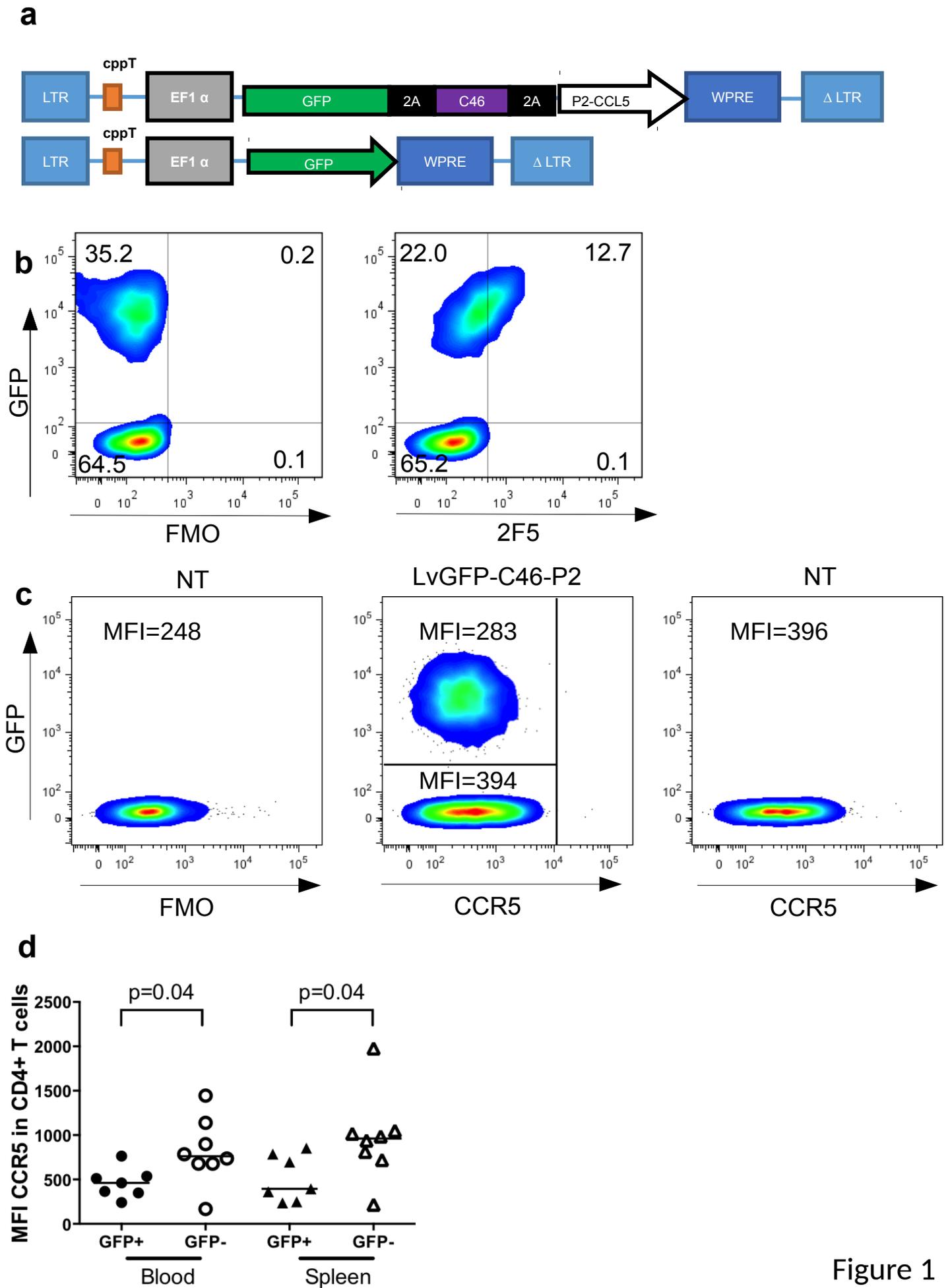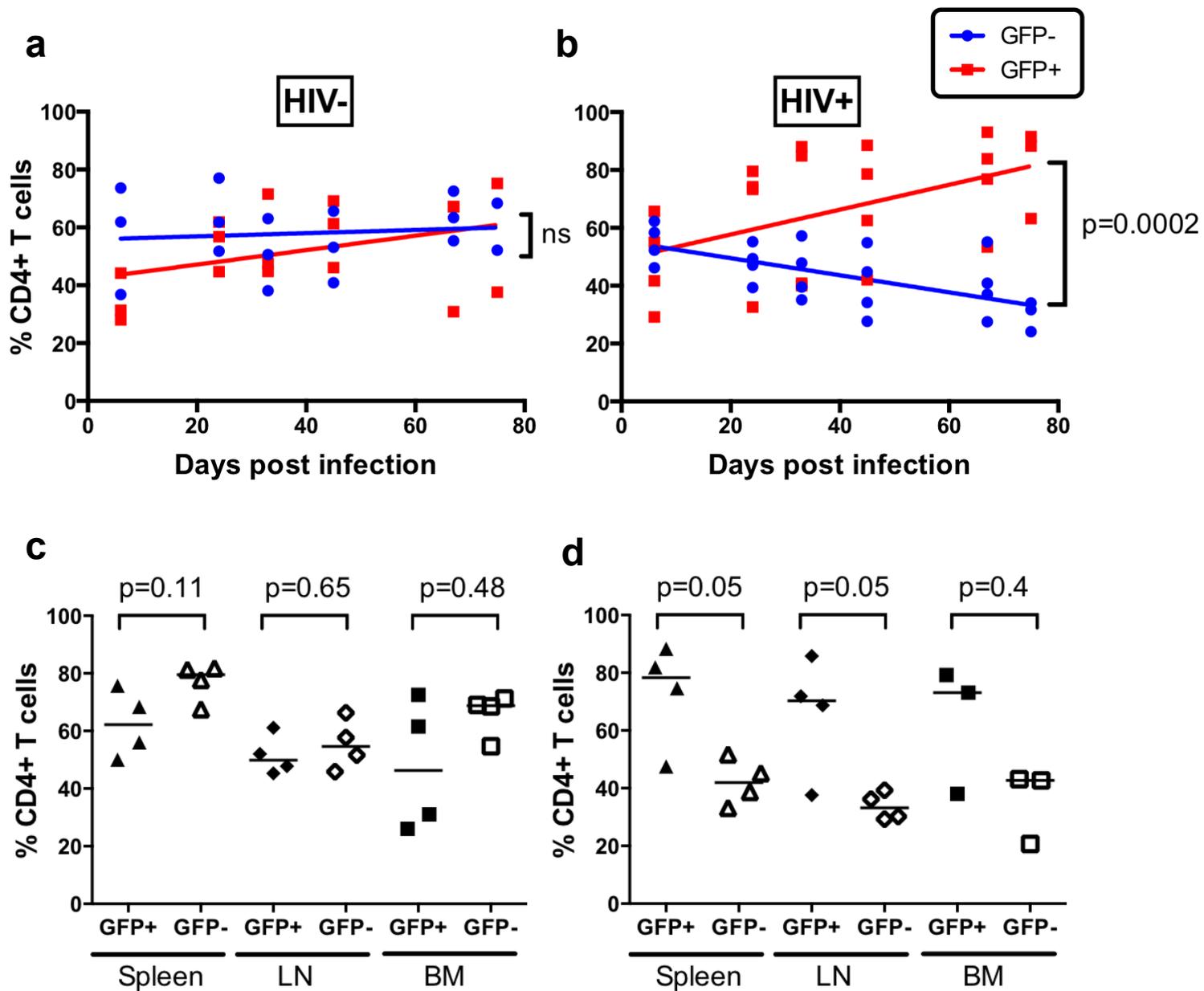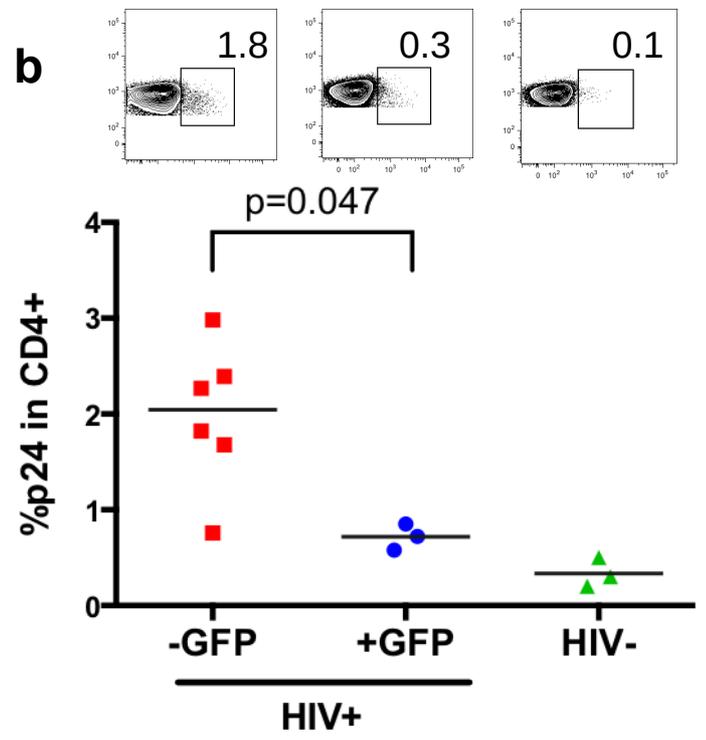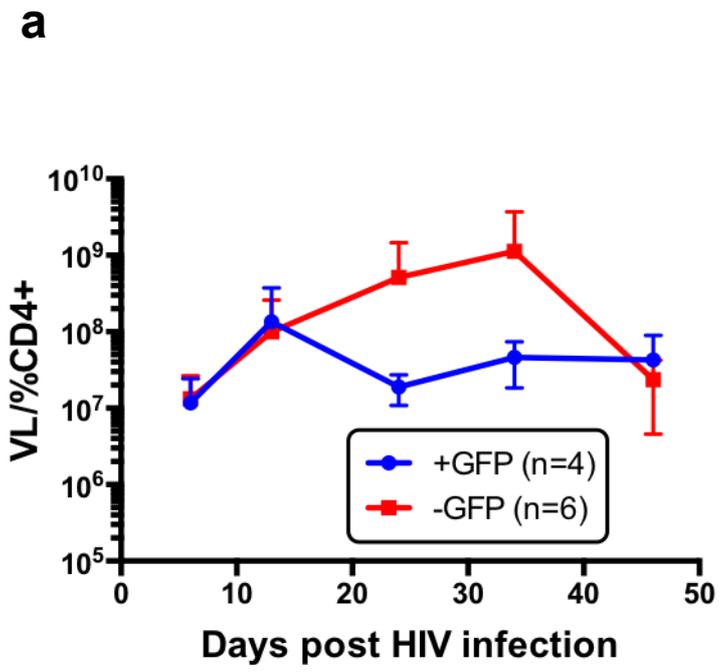
Figure 1

Figure 2

Figure 3

Figure 4